

## Supplementary Information

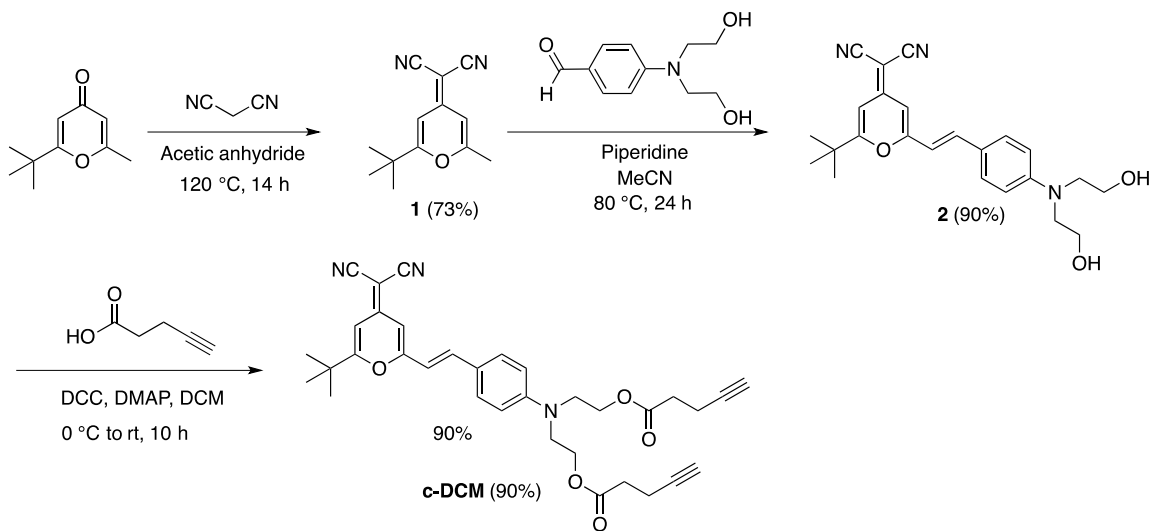
### Sequential “click” functionalization of mesoporous titania for energy-relay dye enhanced dye-sensitized solar cells

Eva L. Unger\*, Samuel J. Fretz, Bogyu Lim, George Y. Margulis, Michael D. McGehee and T. Daniel P. Stack\*

#### S.1 Applying the sequential synthesis to conjugated injecting dyes

In addition to the results described in this work, we attempted the sequential synthesis of conjugated donor-pi-acceptor injecting dyes on mesoporous titanium dioxide by coupling an alkyne-functionalized donor fragment to a surface-bonded azide-functionalized acceptor fragment using the copper(I)-catalyzed azide-alkyne “click” reaction. These attempts were unfruitful as the resulting triazole pi bridge does not provide sufficient conjugation for efficient electron injection. Further information on these results that may be valuable to others trying this approach can be found in the thesis of Samuel J. Fretz.

#### S.2 Dye synthesis and characterization



**Synthesis of 1:** A modified procedure from the literature was used.<sup>1</sup> To a 25 mL round bottom flask was added 2-*tert*-butyl-6-methyl-4H-pyran-4-one (730 mg, 4.40 mmol), malononitrile (436 mg, 6.60 mmol), and acetic anhydride (15 mL). The flask was capped with a rubber septum, purged with N<sub>2</sub> for 15 min., and heated to 120 °C for 14 hrs. After cooling to rt, the brown solution was transferred directly onto a silica gel column and eluted with 1:3 ethyl acetate:hexanes. The product was recrystallized from

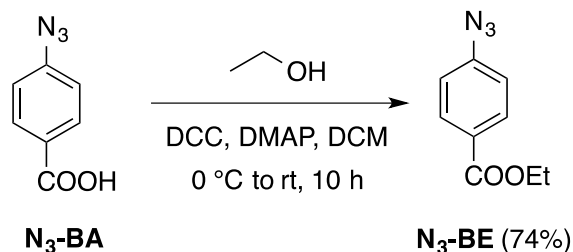
CH<sub>2</sub>Cl<sub>2</sub>/hexanes to yield an off-white solid (940 mg, 73%). <sup>1</sup>H NMR (CDCl<sub>3</sub>, 400 MHz, [ppm]): δ 6.56 (d, 1H, J = 2.07 Hz), 6.55 (m, 1H), 2.34 (d, 3H, J = 0.75 Hz), 1.29 (s, 9H).

**Synthesis of 2:** The solids **1** (530 mg, 2.47 mmol) and 4-[N, N-Bis(2-hydroxyethyl)amino]-benzaldehyde (416 mg, 2 mmol) and a stir bar were placed in a 25 mL Schlenk flask. Under a N<sub>2</sub> atmosphere, dry MeCN (15 mL) and piperidine (100 μL) were added via syringe, and heated at 80 °C for 20 hrs to yield a neon-red solution. The solution was concentrated on a rotary evaporator and the crude product was purified by column chromatography using an ethyl acetate initial eluent, gradually switching to ethyl acetate:methanol mixture of 95:5. The red product fractions were combined, concentrated, and recrystallized from CH<sub>2</sub>Cl<sub>2</sub>:hexanes to yield a bright red powder (730 mg, 90% yield). <sup>1</sup>H NMR (CDCl<sub>3</sub>, 400 MHz, [ppm]): δ 7.42 (d, 2H, J = 8.94 Hz), 7.32 (d, 1H, 15.77 Hz), 6.72 (d, 2H, J = 8.98 Hz), 6.59 (d, 1H, J = 1.98), 6.52 (s, 1H), 6.49 (d, 1H, 13.15 Hz), 3.93 (t, 4H, J = 4.85), 3.69 (t, 4H, J = 5.04), 1.37 (s, 9H). <sup>13</sup>C NMR (CDCl<sub>3</sub>, 400 MHz, [ppm]): δ 172.17, 160.31, 157.06, 150.01, 138.34, 129.97, 123.12, 115.95, 113.53, 112.72, 105.90, 102.65, 60.80, 57.99, 55.36, 36.89, 28.39. LC-MS: m/z 406.20, calculated: 405.49. Elemental analysis calculated for C<sub>24</sub>H<sub>27</sub>N<sub>3</sub>O<sub>3</sub>: C, 71.09; H, 6.71; N, 10.36; Found: C, 71.17; H, 6.71; N, 10.45.

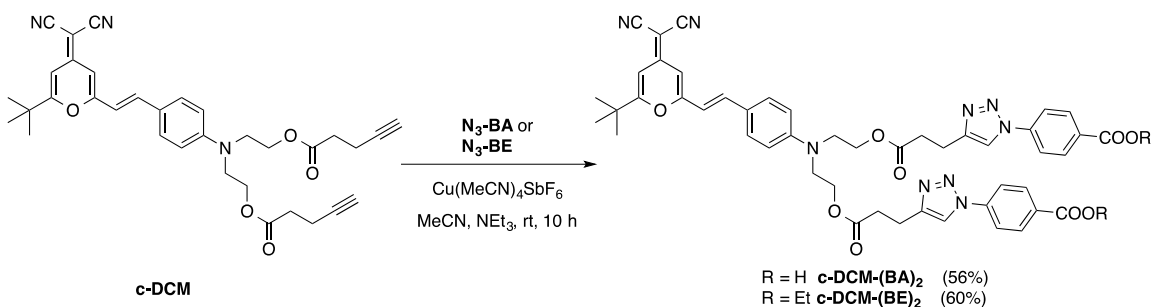
**Synthesis of c-DCM:** The solids **2** (308 mg, 0.76 mmol) and 4-pentynoic acid (223 mg, 2.27 mg) were dissolved in dry CH<sub>2</sub>Cl<sub>2</sub> (25 mL) in a 50 mL rb flask with a stirbar. The flask was capped, cooled to 0 °C, and stirred for 10 min. DCC (463 mg, 2.24 mmol) and DMAP (38 mg, 0.31 mmol) reagents were added in one portion as solids. The mixture was stirred at 0 °C for an additional 10 min. After stirring at rt for 14 hrs, the solution turned to an opaque, red, inhomogeneous mixture. Concentration on the rotary evaporator and purification by column chromatography using 1:1 hexanes:ethyl acetate eluent gave the product as a greasy, red solid. <sup>1</sup>H NMR (CDCl<sub>3</sub>, 400 MHz, [ppm]): δ 7.43 (d, 2H, J = 8.89 Hz), 7.31 (d, 1H, J = 15.82 Hz), 6.77 (d, 2H, J = 8.97 Hz), 6.66 (d, 1H, 2.00 Hz), 6.52 (d, 1H, J = 2.02 Hz), 6.51 (d, 1H, J = 13.82 Hz), 4.31 (t, 4H, J = 6.20 Hz), 3.70 (t, 4H, J = 6.09), 2.58-2.45 (m, 8H), 1.98 (t, 2H, J = 2.51 Hz), 1.37 (s, 9H). <sup>13</sup>C NMR (CDCl<sub>3</sub>, 400 MHz, [ppm]): δ 172.18, 171.89, 160.15, 157.04, 149.29, 138.11, 130.10, 123.61, 115.92, 114.00, 112.31, 106.06, 102.69, 82.49, 69.51, 61.64, 49.72, 34.21, 33.43, 28.39, 25.20, 14.55. LC-MS: m/z 566.20, calculated 565.66. Elemental analysis calculated for C<sub>34</sub>H<sub>35</sub>N<sub>3</sub>O<sub>5</sub>: C, 72.19; H, 6.24; N, 7.43; Found: C, 71.99; H, 7.03; N, 8.04.

The red, oily residue was solidified by initial dissolution in CH<sub>2</sub>Cl<sub>2</sub> in a small vial (20 mL), evaporation under low (100 Torr) then high (100 mTorr) vacuum followed by gently melting of the material. Once completely liquid, the sample was allowed to cool slowly to rt under high vacuum overnight (12-16 hrs), thereby allowing it to crystallize. <sup>1</sup>H NMR spectra before and after the melting process confirmed no degradation of the product.

It should be noted that this compound contained a small quantities of a contaminant, probably N, N'-dicyclohexylurea, as shown in the <sup>1</sup>H NMR (δ 1.95-1.05 ppm). These contaminants persisted despite multiple purifications using column chromatography.



**Synthesis of  $\text{N}_3\text{-BE}$ :** The solids 4-azidobenzoic acid ( $\text{N}_3\text{-BA}$ , 505 mg, 3.10 mmol), DCC (714 mg, 3.46 mmol), and DMAP (38 mg, 0.31 mmol) were placed in a 50 mL rb flask with a stirbar and dry  $\text{CH}_2\text{Cl}_2$  (25 mL). The flask was stirred and cooled at 0 °C for 10 min, followed by dropwise addition of dry ethanol (500  $\mu\text{L}$ , 8.56 mmol). After 10 min, the flask was warmed to rt and stirred for 14 hrs. The opaque, inhomogeneous mixture was placed directly on a silica gel column and eluted with 3:7  $\text{CH}_2\text{Cl}_2$ :hexanes. After concentration on the rotary evaporator, the desired product was isolated as a slightly brown oil that solidified at -20 °C (440 mg, 74%).  $^1\text{H}$  NMR ( $\text{CDCl}_3$ , 400 MHz, [ppm]):  $\delta$  8.03 (app. d, 2H,  $J = 8.32$  Hz), 7.06 (app. d, 2H,  $J = 8.33$  Hz), 4.37 (q, 2H,  $J = 7.13$  Hz), 1.39 (t, 3H,  $J = 6.77$  Hz).



**Synthesis of  $\text{c-DCM-(BA)}_2$ :** In a 20 mL vial was placed **c-DCM** (19 mg, 33  $\mu\text{mol}$ ),  $\text{N}_3\text{-BA}$  (11 mg, 67  $\mu\text{mol}$ ) and a small stir bar. The vial was brought into a  $\text{N}_2$  filled glovebox where  $[\text{Cu}(\text{MeCN})_4]\text{SbF}_6$  (5 mg, 11  $\mu\text{mol}$ ), acetonitrile (5 mL),  $\text{CH}_2\text{Cl}_2$  (5 mL), and triethylamine (200  $\mu\text{L}$ ) were added in that order. The vial was capped and stirred at rt for 10 hrs outside the drybox. The solution contained significant amounts of a solid orange precipitate. The solution/mixture was transferred to a 250 mL separatory funnel where 50 mL of  $\text{CH}_2\text{Cl}_2$ :MeOH:AcOH (90:5:5) and 50 mL  $\text{H}_2\text{O}$  was added. With vigorous shaking the orange solid dissolved in the organic phase. The aqueous layer was reextracted with the same solvent mixture (40 mL) and the two organic layers were combined. After drying with  $\text{MgSO}_4$ , vacuum filtering, washing the  $\text{MgSO}_4$  with an additional 30 mL of  $\text{CH}_2\text{Cl}_2$ :MeOH:AcOH (90:5:5), the light orange solution was concentrated on a rotary evaporator. The crude product was purified by column chromatography ( $\text{SiO}_2$ ) using a short column (3 x 4 cm) eluting with  $\text{CH}_2\text{Cl}_2$ :MeOH:AcOH (95:4:1) to yield the desired compound as an insoluble orange powder (16 mg, 56%). After concentrating the fractions containing orange product, an NMR sample of appropriate concentration was prepared by slow dissolution of ~1 mg of the chromatographed solid into 1.0 mL of  $\text{d}_6\text{-DMSO}$ . Complete dissolution required multiple cycles (4-5) of sonicating and gentle heating. More concentrated NMR samples lead to significantly broadened resonances.  $^1\text{H}$  NMR

(d<sub>6</sub>-DMSO, 400 MHz, [ppm]): 8.56 (br. s, 2H), 8.05 (br. s, 8H), 7.49 (d, 2H, J = 8.34), 7.35 (d, 1H, J = 15.80 Hz), 6.97 (d, 2H, J = 15.41), 6.81 (d, 2H, J = 8.74), 6.68 (s, 1H), 6.37 (s, 1H), 4.19 (br. s, 4H), 3.65 (br. s, 4H), 2.87 (br. s, 4H), 2.65 (br. s, 4H), 1.30 (s, 9H).

Synthesis of c-DCM-(BE)<sub>2</sub>: In a 20 mL vial was placed c-DCM (32 mg, 56 μmol) and a small stir bar. The vial was brought into a N<sub>2</sub> filled glovebox where N<sub>3</sub>-BE (30 μL, 178 μmol), [Cu(MeCN)<sub>4</sub>]SbF<sub>6</sub> (10 mg, 22 μmol), acetonitrile (5 mL), and triethylamine (200 μL) were added in that order. The vial was capped and stirred at rt for 10 hrs outside the drybox. The solution was concentrated on the rotary evaporator and the red residue was purified via column chromatography using a 98:2 CH<sub>2</sub>Cl<sub>2</sub>:methanol eluent. After concentration, the product was recrystallized from CH<sub>2</sub>Cl<sub>2</sub>:hexanes to yield the desired product as a red powder (32 mg, 60%). <sup>1</sup>H NMR (CDCl<sub>3</sub>, 400 MHz, [ppm]): 8.18 (app. d, 4H, J = 8.84 Hz), 7.85 (s, 2H), 7.78 (app. d, 4H, J = 8.78 Hz), 7.37 (d, 2H, J = 8.95 Hz), 7.28 (d, 1H, J = 15.53 Hz – other half of doublet obscured by CHCl<sub>3</sub>), 6.73 (d, 2H, J = 8.91 Hz), 6.59 (d, 1H, J = 2.03 Hz), 6.52 (d, 1H, J = 2.05 Hz), 6.47 (d, 1H, J = 15.87 Hz), 4.41 (q, 4H, J = 7.16 Hz), 4.29 (t, 4H, J = 5.96 Hz), 3.68 (t, 4H, J = 6.18 Hz), 3.09 (t, 4H, J = 7.21 Hz), 2.81 (t, 4H, J = 7.13 Hz), 1.42 (t, 6H, J = 7.16 Hz), 1.37 (s, 9H).

General procedure employed for the CH<sub>2</sub>Cl<sub>2</sub>/hexanes recrystallization: The crude product was dissolved completely in a minimal amount of CH<sub>2</sub>Cl<sub>2</sub> followed by dilution with hexanes (typically 1-1.5x the volume of CH<sub>2</sub>Cl<sub>2</sub>). After thorough mixing of the solution, the flask containing the solution was placed on the rotary evaporator under light vacuum (~100 Torr) to slowly remove the CH<sub>2</sub>Cl<sub>2</sub> component of the solvent mixture. Once the majority of CH<sub>2</sub>Cl<sub>2</sub> had evaporated, the product crystallized. This product was filtered, washed with hexanes, and dried open to the air.

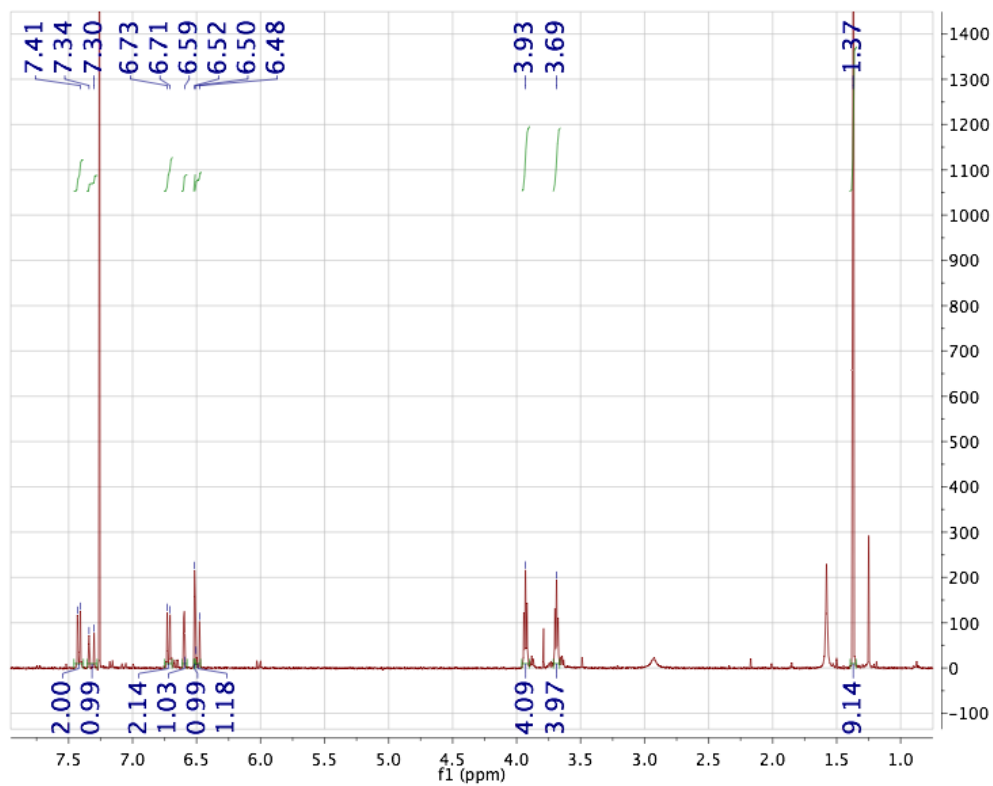


Figure S1  $^1\text{H}$  NMR of 2.

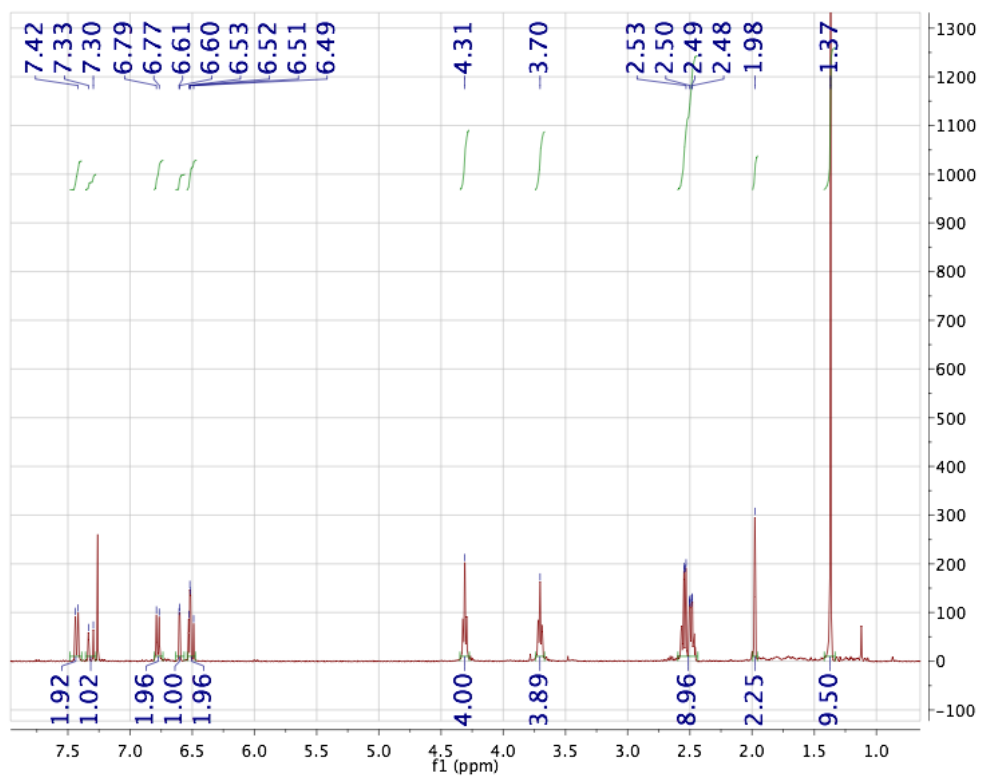


Figure S2  $^1\text{H}$  NMR of c-DCM.

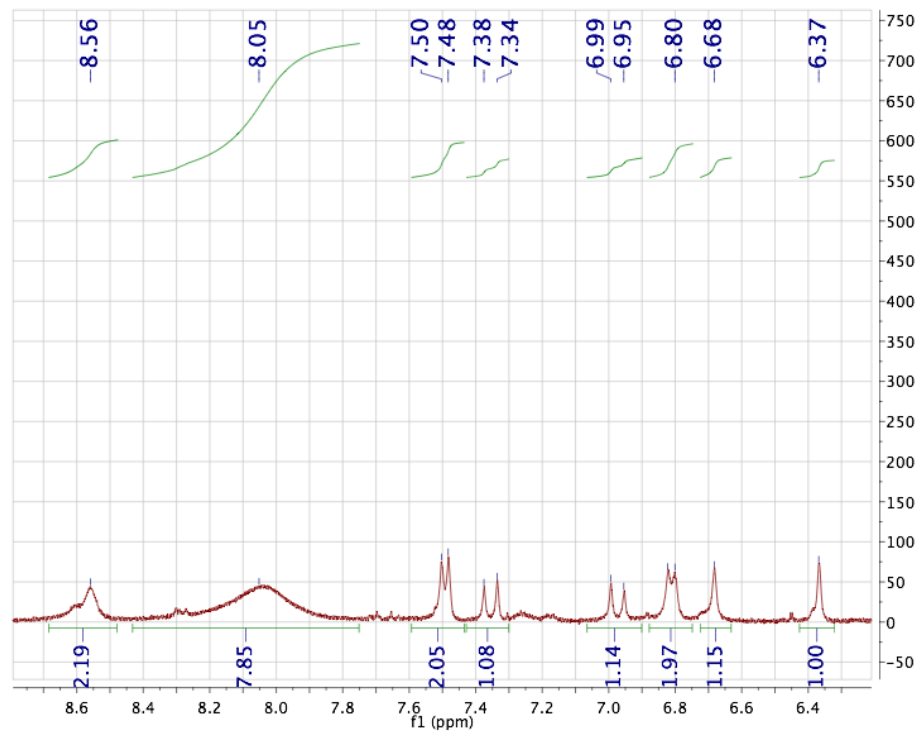


Figure S3 <sup>1</sup>H NMR of the aromatic region of c-DCM-(BA)<sub>2</sub>.

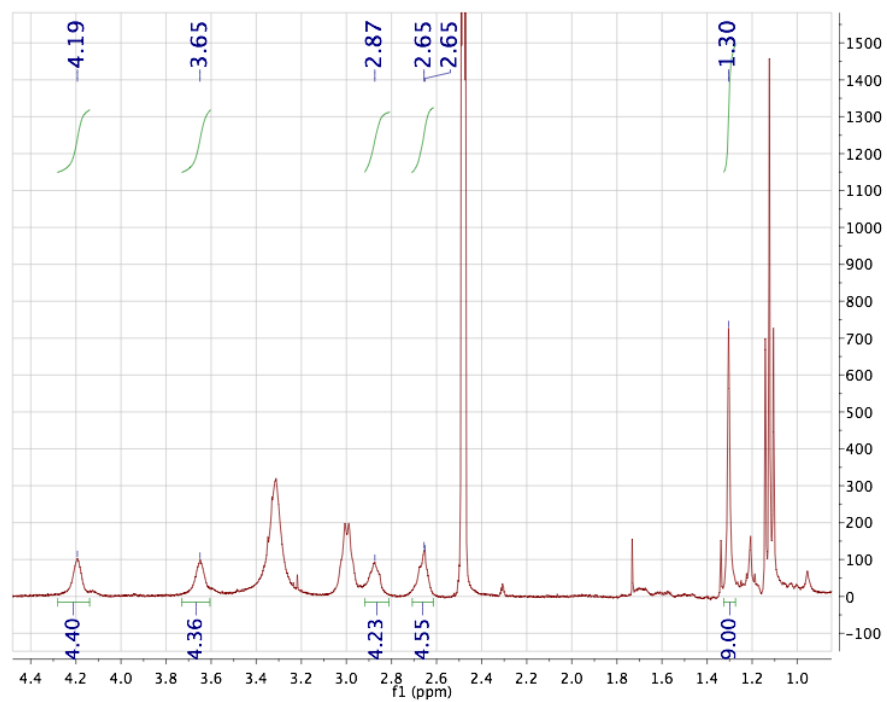


Figure S4 <sup>1</sup>H NMR of the aliphatic region of c-DCM-(BA)<sub>2</sub>.

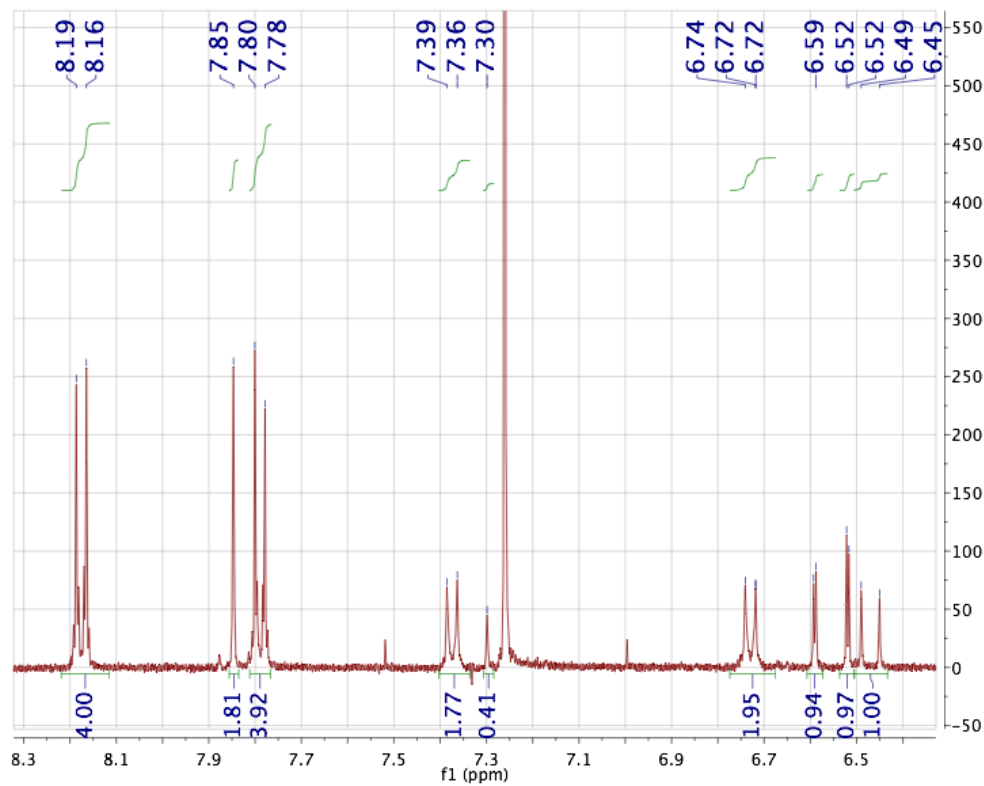


Figure S5 <sup>1</sup>H NMR of the aromatic region of c-DCM-(BE)<sub>2</sub>.

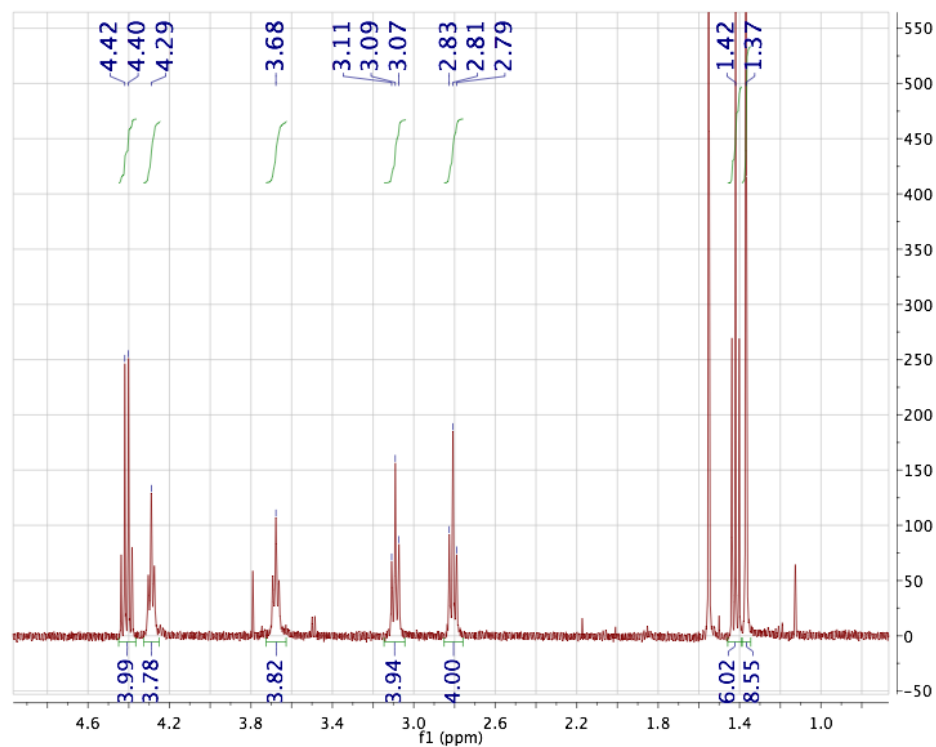
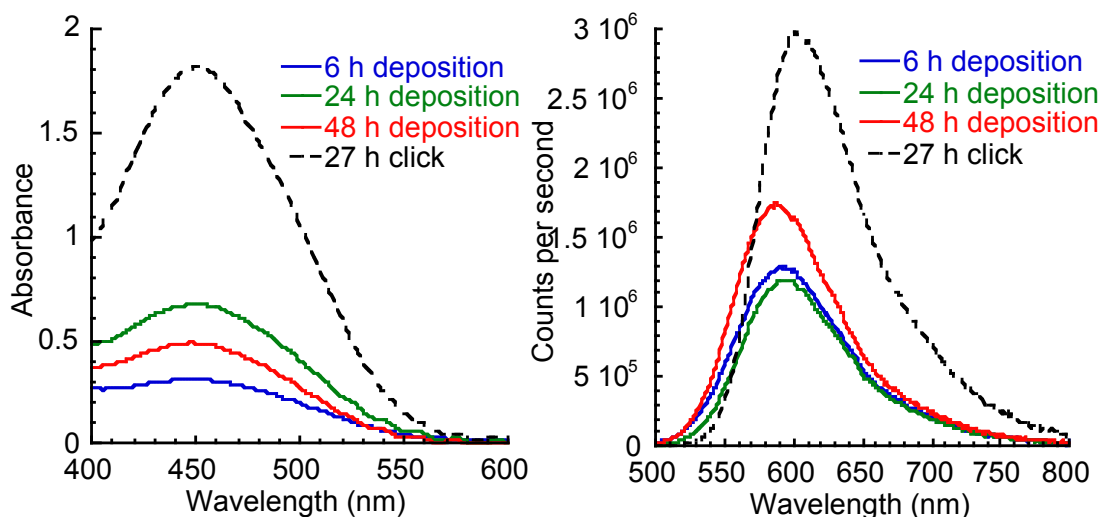


Figure S6 <sup>1</sup>H NMR of the aliphatic region of c-DCM-(BE)<sub>2</sub>.

### S.3 Chemisorption of **c-DCM-(BA)<sub>2</sub>** to mesoporous TiO<sub>2</sub>

The highly insoluble nature of **c-DCM-(BA)<sub>2</sub>** makes comparison to the surface-clicked **c-DCM** difficult. The slides were immersed in a 0.1 mM DMSO solution of **c-DCM-(BA)<sub>2</sub>** for 6, 24, or 48 hrs. Afterwards, the slides were rinsed with DMSO, the 1:10 diluted electrolyte solution, and MeCN and dried in an N<sub>2</sub> steam. The transmission UV-Vis spectra and front-face fluorescence spectra are shown in in Figure S7. The surface-clicked sample (27 h click) is shown for comparison in the dotted black trace.



**Figure S7** Transmission UV-Vis spectra (left) and front-face fluorescence spectra (right) after the deposition of **c-DCM-(BA)<sub>2</sub>**. A surface-clicked sample is shown for comparison (black dashed trace).

Significantly higher amounts of **c-DCM** can be immobilized on the surface using the two-step sequential method compared with the traditional one-step deposition. While the maximum amount of **c-DCM-(BA)<sub>2</sub>** on the surface varied between experiments, the maximum absorbance value never rose above 0.9 absorbance units; the click method immobilizes more than 2x the amount of **c-DCM**.

## S.4 Optical and electrochemical characterization

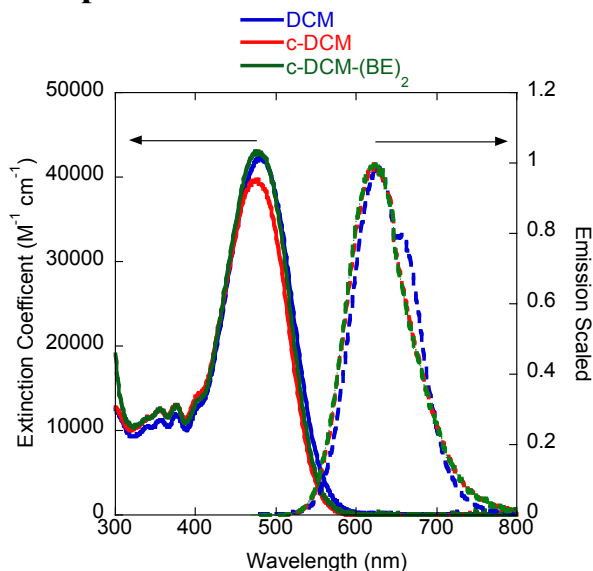


**Figure S8** Absorption (solid) and emission (dashed) spectra of **DCM** (blue), **c-DCM** (red), and **c-DCM-(BE)<sub>2</sub>** (green) in DMSO ( $10^{-5}$  M for absorption spectra,  $10^{-6}$  M for emission spectra).

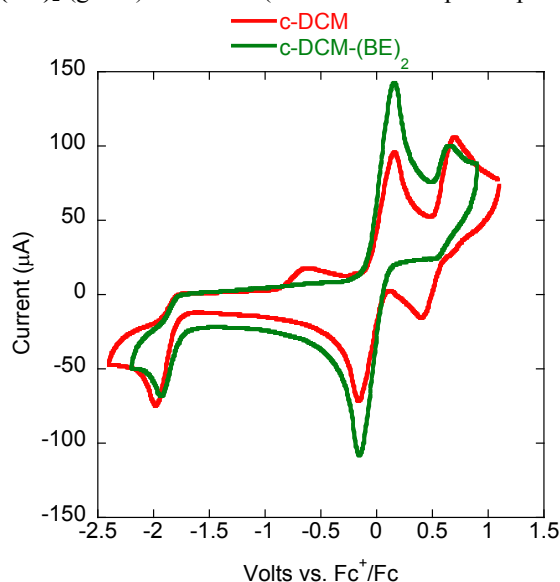


**Figure S9:** Cyclic voltammograms of **c-DCM** (red) and **c-DCM-(BE)<sub>2</sub>** (green) in  $\text{CH}_2\text{Cl}_2$  with 100 mM (n-Bu)<sub>4</sub>N-BF<sub>4</sub> as the supporting electrolyte and ferrocene (Fc) as the internal reference.

The redox potentials of **c-DCM** and **c-DCM-(BE)<sub>2</sub>** were determined to be 0.55 V and 0.58 V vs  $\text{Fc}^+/\text{Fc}$ , respectively. Using reference values of +0.52 V vs  $\text{Ag}/\text{AgCl}/\text{KCl}(\text{sat.})$  for the  $\text{Fc}^+/\text{Fc}$  redox couple in  $\text{CH}_2\text{Cl}_2$  solution<sup>2</sup>, 0.198 V of  $\text{Ag}/\text{AgCl}/\text{KCl}(\text{sat.})$  vs NHE, the oxidation potentials vs NHE were estimated to be 1.27 V and 1.30 V for **c-DCM** and **c-DCM-(BE)<sub>2</sub>**, respectively.

## S.5 First batch of devices: Dissolution of agglomerates

The first batch of solar cell devices functionalized with **SQ02** and **c-DCM** using the sequential functionalization approach exhibited very low device performance despite high light harvesting efficiency expected for both dyes from the UV-Vis absorption measurements of full devices. **SQ02** only devices with a  $N_3$ -BA diluent were investigated for reference which gave up to 40% of external quantum efficiency comparable to results published elsewhere.<sup>3</sup>

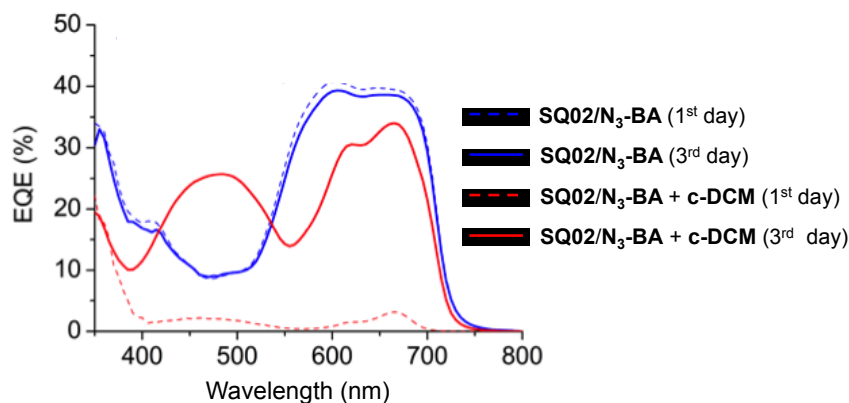


**Figure S10** External quantum efficiency (EQE) spectra of DSCs containing **SQ02** and  $N_3$ -BA diluent (blue) and with **c-DCM** (red). The dashed traces are EQE spectra immediately after construction of the device and the solid traces after three days.

After three days of storage, device performance increased by a factor of 10. The electrolyte solution in the device exhibited a dark-orange color, suggesting dissolution of some type of **c-DCM** agglomerates from the mesoporous scaffold into the DSC electrolyte solution. These reactant agglomerates formed during the click-reaction functionalization step within the mp- $TiO_2$  scaffold inhibit dye-regeneration giving rise to low internal quantum efficiencies of the dye molecules. These agglomerates were not removed by rinsing with pure acetonitrile (MeCN) but are soluble in the MeCN electrolyte solutions used to create DSCs. A rinsing step with diluted MeCN electrolyte solution was therefore introduced after the click-reaction step.

## S.6 SQ02 concentration as function of $N_3$ -BA co-adsorber

In Figure S11, the absorbance of meso-porous  $TiO_2$  sample (thickness *ca.* 2  $\mu m$ ) is shown for samples sensitized with increasing amounts of  $N_3$ -BA in the solution. The relative amount of squaraine dye decreases with increasing co-adsorber concentration similar to results using cheno-deoxycholic acid as the co-adsorber.<sup>4</sup> Using the integrated spectrum to account for changes in absorbance due to aggregate formation, the addition of 1, 5 and 10 mM  $N_3$ -BA reduces the SQ02 surface concentration decreases by 53%, 72% and 83% respectively.

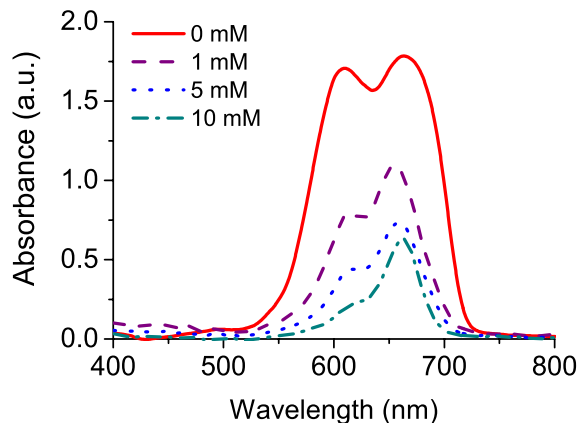


**Figure S11** UV-vis absorption spectra of 2  $\mu\text{m}$  mesoporous  $\text{TiO}_2$  samples sensitized with 0 mM, 1 mM, 5 mM and 10 mM  $\text{N}_3\text{-BA}$  in the dye-solution.

### S.7 Light harvesting and energy transfer efficiency

To determine the light harvesting efficiency of the ERD and ID within the solar cell device geometry, the absorbance of the entire device was measured in an integrating sphere. To account for parasitic absorption losses only in the front electrode and within the meso-porous  $\text{TiO}_2$  the absorbance of a meso-porous  $\text{TiO}_2$  film of similar thickness on conducting FTO, stained with electrolyte solution and covered with a thin cover slip was measured. From the EQE data shown in Figure 5, the ETE can then be calculated accordingly, taking parasitic absorption losses at the respective wavelength of ERD response and ID response into account.

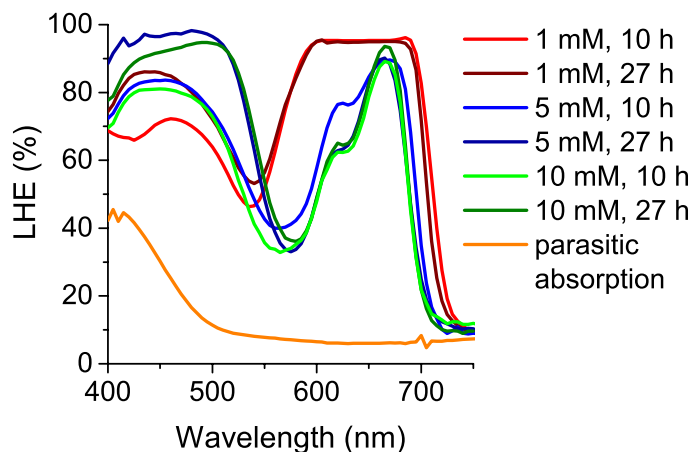


**Figure S12** Light harvesting efficiency of solar cell devices measured on devices within an integrating sphere, the parasitic absorption loss of light absorbed in the front electrode is shown for reference.

## S.8 Comparison with other reported ERD-enhanced DSCs

For comparison of the relative device efficiency improvement achieved herein, we compiled the following table, summarizing other reports on energy relay dye enhanced DSCs.

**Table S1: Comparison of relative device improvement in reported ERD-enhanced DSC devices**

Reference	ERD	ID	LHE <sub>ERD</sub>	R <sub>0,DA</sub>	ETE	EQE <sub>ERD</sub> <sup>a</sup>	Δη
Siegers <i>et al.</i> , 2007 <sup>5</sup> (dyadic)	Fluorol 7GA	[Ru(dcbpy) <sub>2</sub> (acac)]Cl	95%	4.6 nm	85%	10%	+9%
Siegers <i>et al.</i> , 2008 <sup>6</sup> (dyadic)	CF	N719	58%	n.a.	89%	9%	-5%
Hardin <i>et al.</i> , 2009 <sup>7</sup>	PTCDI	TT1	90%	8 nm	47%	29%	+26%
Hardin <i>et al.</i> , 2010 <sup>8</sup>	DCM	TT1	39%	6.9 nm	96%	28%	+29%
Mor <i>et al.</i> , 2010 <sup>9</sup> (solid state DSC)	DCM	SQ01	ca. 80%	6.1 nm	68%	22%	+82%
Yum <i>et al.</i> , 2011 <sup>10</sup>	DCM RB	TT1	ca. 40% 79%	6.9 nm 6.3 nm	95% 34%	27% 19%	+25% +12%
Brown <i>et al.</i> , 2011 <sup>11</sup> (surface-bonded)	D102	TT1	80%	3.5 nm	50%	14%	+21%
Shrestha <i>et al.</i> , 2012 <sup>12</sup>	BET	LD12	n.a.	n.a.	n.a.	30%	+13%
Margulis <i>et al.</i> , 2013 <sup>1</sup>	BL302 BL315	TT1 TT1	97%	6.0 nm	70% 67%	55% 45%	+51% +56%
Gao <i>et al.</i> , 2014 <sup>13</sup> (quasi-solidstate)	DCJTb	N3	55%	5.2 nm	>50%	23%	+32%
Yun <i>et al.</i> , 2015 <sup>14</sup> (quasi-solid state)	DCM	SQ-dye	n.a.	n.a.	n.a.	28%	+77%
This work (immobilized)	c-DCM- (BA) <sub>x</sub>	SQ02	ca. 100%	6.1 nm	85%	42% 38%	+61% +124%

<sup>a</sup> EQE<sub>ERD</sub> is the additional external quantum efficiency response from light harvested in the energy relay dye. <sup>b</sup> Δη is the relative efficiency improvement of ERD-enhanced DSC with respect to a reference device without ERD.

## S.9 Photoluminescence of SQ02/c-DCM functionalized ZrO<sub>2</sub> films

We did a complementary experiment where we measured the photoluminescence of meso-porous zirconia samples (thickness *ca.* 2 μm) that were functionalized in two sequential steps with different solution concentrations of **N<sub>3</sub>-BA** (0, 1, 5 and 10 mM) and a reaction time of 24 hours in the second step. The photoluminescence was corrected for the difference in light harvesting efficiency at the excitation wavelength of 450 nm. Qualitatively, at low **N<sub>3</sub>-BA** surface concentrations no photoluminescence from the surface-bonded **c-DCA-(BA)<sub>x</sub>** is observed while residual emission from **c-DCA-(BA)<sub>x</sub>** can be observed for an increased surface concentration of **N<sub>3</sub>-BA**. In this case it can be expected, that the relative distance between the ERD and nearest ID is larger and the ETE therefore slightly reduced. The relative high PL observed from the ERD indicates that self-quenching of ERD immobilized to the surface is not a big issue which is consistent with the relatively small spectral self-overlap of the ERD.

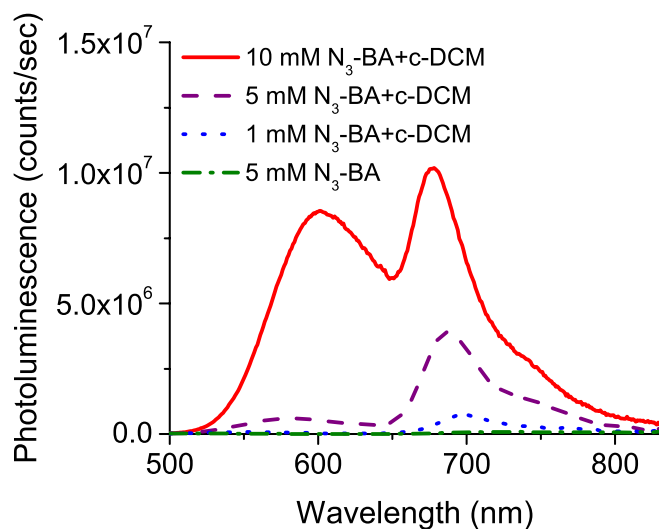


**Figure S13** Photoluminescence of ca. 2  $\mu\text{m}$  thick mesoporous  $\text{ZrO}_2$  samples functionalized with **SQ02** and **c-DCM** equivalent to other samples described in this work.

## References

- (1) Margulis, G. Y.; Lim, B.; Hardin, B. E.; Unger, E. L.; Yum, J.-H.; Feckl, J. M.; Fattakhova-Rohlfing, D.; Bein, T.; Grätzel, M.; Sellinger, A.; McGehee, M. D. *Phys. Chem. Chem. Phys.* **2013**, *15*, 11306–11312.
- (2) Noviandri, I.; Brown, K. N.; Fleming, D. S.; Gulyas, P. T.; Lay, P. A.; Masters, A. F.; Phillips, L. J. *Phys. Chem. B* **1999**, *103*, 6713–6722.
- (3) Geiger, T.; Kuster, S.; Yum, J.-H.; Moon, S.-J.; Nazeeruddin, M. K.; Grätzel, M.; Nüesch, F. *Adv. Funct. Mater.* **2009**, *19*, 2720–2727.
- (4) Yum, J. H.; Moon, S. J.; Humphry-Baker, R.; Walter, P.; Geiger, T.; Nüesch, F.; Grätzel, M.; Nazeeruddin, M. D. K. *Nanotechnology* **2008**, *19*, 424005.
- (5) Siegers, C.; Hohl-Ebinger, J.; Zimmermann, B.; Würfel, U.; Mülhaupt, R.; Hinsch, A.; Haag, R. *Chemphyschem* **2007**, *8*, 1548–1556.
- (6) Siegers, C.; Würfel, U.; Zistler, M.; Gores, H.; Hohl-Ebinger, J.; Hinsch, A.; Haag, R. *Chemphyschem* **2008**, *9*, 793–798.
- (7) Hardin, B. E.; Hoke, E. T.; Armstrong, P. B.; Yum, J.-H.; Comte, P.; Torres, T.; Fréchet, J. M. J.; Nazeeruddin, M. K.; Grätzel, M.; McGehee, M. D. *Nat. Photonics* **2009**, *3*, 406–411.
- (8) Hardin, B. E.; Yum, J.-H.; Hoke, E. T.; Jun, Y. C.; Péchy, P.; Torres, T.; Brongersma, M. L.; Nazeeruddin, M. K.; Grätzel, M.; McGehee, M. D. *Nano Lett.* **2010**, *10*, 3077–3083.
- (9) Mor, G. K.; Basham, J.; Paulose, M.; Kim, S.; Varghese, O. K.; Vaish, A.; Yoriya, S.; Grimes, C. A. *Nano Lett.* **2010**, *10*, 2387–2394.

- (10) Yum, J.-H.; Hardin, B. E.; Hoke, E. T.; Baranoff, E.; Zakeeruddin, S. M.; Nazeeruddin, M. K.; Torres, T.; McGehee, M. D.; Grätzel, M. *Chemphyschem* **2011**, *12*, 657–661.
- (11) Brown, M. D.; Parkinson, P.; Torres, T.; Miura, H.; Herz, L. M.; Snaith, H. J. **2011**, 23204–23208.
- (12) Shrestha, M.; Si, L.; Chang, C.-W.; He, H.; Sykes, A.; Lin, C.-Y.; Diau, E. W.-G. *J. Phys. Chem. C* **2012**, *116*, 10451–10460.
- (13) Gao, R.; Cui, Y.; Liu, X.; Wang, L. *Sci. Rep.* **2014**, *4*, 5570.
- (14) Yun, H. J.; Jung, D. Y.; Lee, D. K.; Jen, A. K.-Y.; Kim, J. H. *Dye. Pigment.* **2015**, *113*, 675–681.